Acta Geologica Sinica (English Edition), 2020, 94(1): 210–211

Research Advances

New $^{40}Ar/^{39}Ar$ Data of Gold Mineralization in the Ailaoshan Gold Belt, Yunnan Province, China

YANG Zongyao[1], HU Guyue[2,*] and ZHAO Xiaoyan[1]

[1] *Faculty of Geosciences and Environmental Engineering, Southwest Jiaotong University, Chengdu 610059, China*
[2] *MNR Key Laboratory of Metallogeny and Mineral Assessment, Institute of Mineral Resources, CAGS, Beijing China*

Citation: Yang et al., 2020. New $^{40}Ar/^{39}Ar$ Data of Gold Mineralization in the Ailaoshan Gold Belt, Yunnan Province, China. Acta Geologica Sinica (English Edition), 94(1): 210–211. DOI: 10.1111/1755-6724.14415

Objective

"Orogenic gold deposits," which account for 30 % of global gold resources (Frimmel and Hennigh, 2015), is one of the most important types of gold deposits in the world. This kind of gold deposit is supposed to have spatial and temporal distribution association with the accretionary orogenic belt. The Ailaoshan Gold Belt, where there are many large orogenic gold deposits including Jinchang, Daping, Laowangzhai, Donggualing, and Changan, contribute substantially to Chinese gold resources. The Himalayan orogen and Ailaoshan Orogen, both have experienced the early accretionary orogenesis and the subsequent collisional orogenesis are one of the biggest orogenic belts on the earth. Gold mineralization can be divided into that the earlier Yarlung Zangbo suture zone (59–44 Ma) and the later Ailaoshan Orogen (35–26 Ma) (Li et al., 2017), based on previous geochronological studies. In order to find out if there are any connections between these two gold events, we present $^{40}Ar/^{39}Ar$ data of hydrothermal sericite collected from the Xiachahe gold deposit in the northwest of the Ailaoshan Gold Belt. However, our new geochronology data regards this as a continuous gold mineralization event resulting from the India–Eurasia collision.

Methods

Auriferous quartz, mylonite, and ultramylonite samples were collected from orebody II in Channel CM 1 (Fig.1a) and crushed and sieved sizes of 40 to 60 mesh. Hydrothermal sericite selected for $^{40}Ar/^{39}Ar$ dating was extracted from the crushed samples via the floatation method and were then carefully handpicked to a purity of more than 99 % under a microscope. The hydrothermal sericite was firstly cleaned via ultrasonic treatment under ethanol. Second, about 3 mg hydrothermal sericite was packaged and put in a vacuum. Third, this prepared hydrothermal sericite was irradiated with fast neutrons for nearly 55 h in the H8 nuclear reactor at the Chinese Academy of Atomic Energy. The monitor irradiated in this study was an internal standard denoted Fangshan biotite (ZBH-25), with an age of 132.7 Ma and a potassium content of 7.6%.

* Corresponding author. E-mail: wanghuguyue@126.com

The $^{40}Ar/^{39}Ar$ test was finished with a Helix SFT noble gas mass spectrometer at the Analytical Laboratory, Beijing Research Institute of Uranium Geology, China National Nuclear Corporation, using the step-heating $^{40}Ar/^{39}Ar$ method. The decay constant of ^{40}K used in the calculation was $\lambda = 5.543 \times 10^{-10}$/year. Age errors are quoted at a 1σ confidence level. Argon isotope ratios are presented on isochron diagram using the ISOPLOT program (ver. 3.0) in Microsoft Excel.

Results

The results of the $^{40}Ar/^{39}Ar$ analysis of hydrothermal sericite are listed in Appendix 1. Nine steps from 760 to 1400 °C on the on the age-heating spectrum of hydrothermal sericite sample yielded a plateau age of 43.68±0.32 Ma (Fig. 1b) and a normal isochronal age of 43.16±0.35 Ma (Fig. 1c). In addition, the K-Ar isotopic system of the samples were not affected by heating because a high amount of ^{39}Ar (93.11%) was released. The plateau age is nearly the same as the normal isochronal age, indicating that the data is reliable.

Conclusion

The hydrothermal sericite from the Xiachahe gold deposit with an $^{40}Ar/^{39}Ar$ plateau age of 43.68±0.32 Ma, which indicates that the metallogenic age of samples from the Xiachahe gold deposit can be earlier than 43 Ma. Therefore, the gold mineralization in the Ailaoshan Gold Belt could have happened as early as the middle Eocene, which is different from the previous point of Li et al. (2017). Another notable point is that the age of the Xiachahe gold deposit is nearly the same as that of the hydrothermal sericite $^{40}Ar/^{39}Ar$ (44 Ma) from the Bangbu gold deposit in the eastern Yarlung Zangbo suture zone (Sun et al., 2016). The mineralization of gold from the western of Yarlung Zangbo suture zone, which is southeast of the Ailaoshan Gold Belt, seems to have occurred in order from 59 Ma to 26 Ma. This means that the area between the Yarlung Zangbo suture zone and Ailaoshan Gold Belt should be a new direction for gold prospecting, because it might be possible to find an orogenic gold deposit there that formed from approximately 44 Ma to 35 Ma.

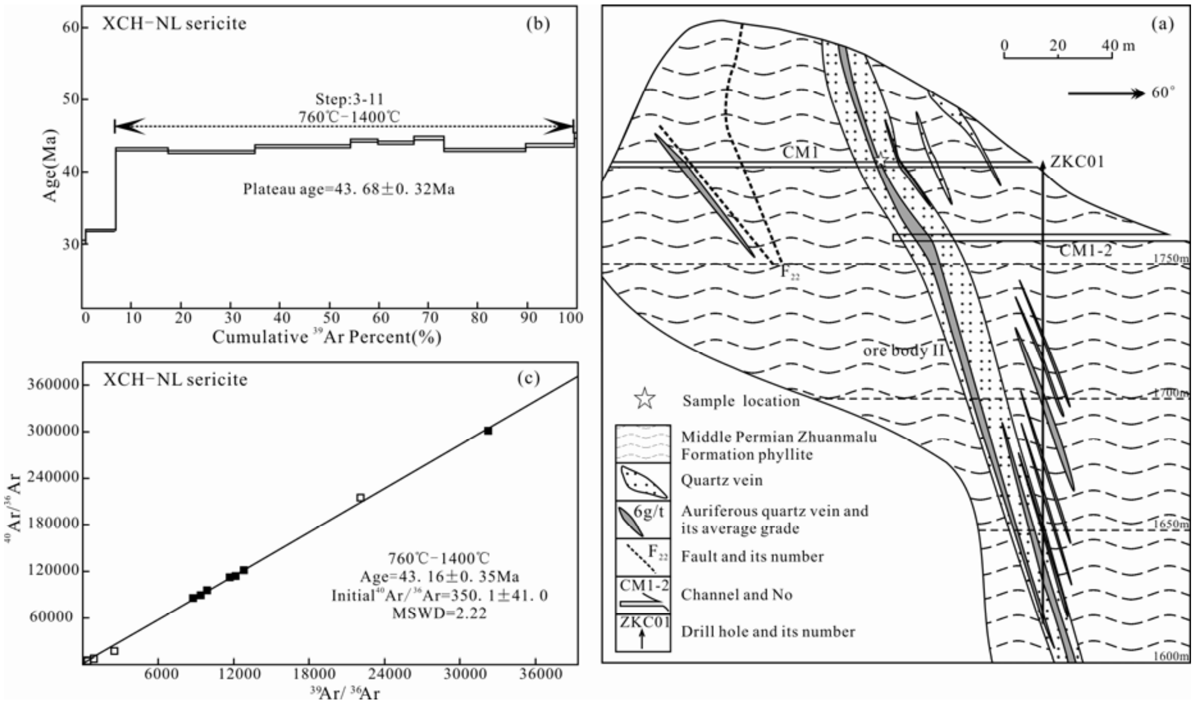

Fig. 1. Cross section (a); Plateau (b) and isochrona age (c) of hydrothermal sericite from auriferous quartz vein.

Acknowledgments

This study was supported by the National Science Foundation of China (grant No. 41772075) and the National Key R&D Program of China, Deep Resources Exploration and Mining (grant No. 2018YFC0604105).

References

Frimmel, H.E., and Hennigh Q., 2015. First whiffs of atmospheric oxygen triggered onset of crustal gold cycle. Mineralium Deposita, 50: 5–23.

Li, H.J., Wang, Q.F., Yang L., Yu, H.Z., and Wang, X., 2017. Orogenic gold deposits formed in Tibetan collisional orogen setting: Geotectonic setting, geological and geochemical features. Acta Petrologica Sinica, 33(7): 2189–2201 (in Chinese with English abstract).

Sun, X.M., Wei, H.X., Zhai, W., Shi, G.Y., Liang Y.H., Mo, R.W, Han, M.X., Yi, J.Z., and Zhang, X.G., 2016. Fluid inclusion geochemistry and Ar–Ar geochronology of the Cenozoic Bangbu orogenic gold deposit, southern Tibet, China. Ore Geology Reviews, 74: 196–210

Appendix 1 $^{40}Ar/^{39}Ar$ data of hydrothermal sericite from Xiachahe gold deposit.

T(℃)	$^{40}Ar/^{39}Ar$	$^{36}Ar/^{39}Ar$	$^{37}Ar/^{39}Ar$	^{40}Ar(%)	F($^{40}Ar^*/^{39}Ar$)	^{39}Ar ($\times 10^{-14}$mol)	^{39}Ar (Cum.)(%)	Age (Ma)	±1σ (Ma)
630	6.924	0.00114	0.0002	95.1	6.5848	0.47	0.8	30.26	0.26
710	7.0555	0.0004	0.0009	98.29	6.935	3.58	6.08	31.86	0.16
760	9.4584	0.00011	0.0006	99.66	9.4258	6.18	10.51	43.16	0.21
810	9.3498	0.00003	0.0005	99.89	9.3394	10.31	17.54	42.77	0.21
860	9.5268	0.00008	0.0008	99.74	9.5025	11.36	19.34	43.51	0.22
910	9.7014	0.00005	0.0003	99.85	9.6869	3.23	5.5	44.34	0.22
960	9.6478	0.0001	0.0000	99.68	9.6168	4.28	7.29	44.03	0.22
1010	9.8023	0.00011	0.0003	99.64	9.7673	3.61	6.15	44.71	0.22
1100	9.4286	0.00008	0.0001	99.73	9.4031	9.69	16.49	43.06	0.21
1200	9.5709	0.00009	0.0003	99.72	9.5445	5.76	9.8	43.7	0.22
1400	12.2753	0.00825	0.0554	80.17	9.8419	0.29	0.5	45.05	0.43